Active photonic integrated circuits using semiconductor optical amplifiers

Yiwei Xie, Leimeng Zhuang, Arthur James Lowery
Electro-Photonics Laboratory, Dept. of Elec. and Computer Sys. Eng., Monash University, Wellington Road, Clayton, Australia
yiwei.xie@monash.edu; leimeng.zhuang@monash.edu; arthur.lowery@monash.edu

Abstract— **Active photonic circuits use combinations of active semiconductor devices and passive elements to support many applications. We present four functions on a single active photonic integrated circuit (4.5 mm × 4 mm).**

Keywords-Integrated photonic circuits; ring resonator; semiconductor optical amplifier

I. Introduction

Photonic signal processing, using photonic approaches to condition optical signals, offers advantages of large time-bandwidth capabilities to overcome inherent electronic speed limitations, and immunity to electromagnetic interference (EMI) [1]. Active Photonic Circuits [2] combine active semiconductor devices and passive elements to provide novel functionality, such as high-speed demultiplexing, microwave photonics [3], optical packet switching and optical instrumentation [4]. The active element is usually a semi-conductor optical amplifier (SOA), as SOAs have advantages of high optical gain per unit length, and can be switched using their injection current. To date, most of the applications using SOAs have been realized by discrete optical components, having their optical paths connected using optical fibers [3-4].

In this paper, we present a new photonic integrated circuit (PIC) design using indium phosphide (InP) technology, in which the key optical element is a SOA. We have demonstrated the PIC's functions include: delay discriminator, optical sampler, tunable delay line, and wavelength converter.

II. Overview of the PIC

Lowery [2] analyzed and simulated many photonic integrated circuits based on SOAs in 2005, four applications are shown in Fig. 1a. We have designed and developed these topologies onto a PIC, which has been fabricated via the JePPIX foundry service using SMART Photonics' InP platform (Fig. 1b). This has shallow-etched InP waveguides with a propagation loss of 3.5 dB/cm and coupling loss of about 4 dB from a facet to a lensed fiber. We have used the structures on the PIC, and demonstrated four separate functions, described in the next section.

III. Applications of the PIC

We have characterized various parts of the chip and shown their utility in several applications, described below.

A. Delay discriminator

The comparison of the arrival times of modulated optical waveforms is critical to the design of all-optical clocks using phase-locked loops. The delay discriminator was first proposed by Lowery and Premaratne in 2005 [5], we have developed and demonstrated this device in [6]. Part 2 in Fig. 1c shows the structure of the device, which contains a serial cascade of three sections of SOAs and two integrated photodiodes (PD). Forward and backward propagating pulse are injected into a cascade of three sections of SOAs from opposite sides. The left- and right-facet output signals of the SOA are individually detected by PDs. If a forward-propagating pulse leads a backward-propagating pulse, then

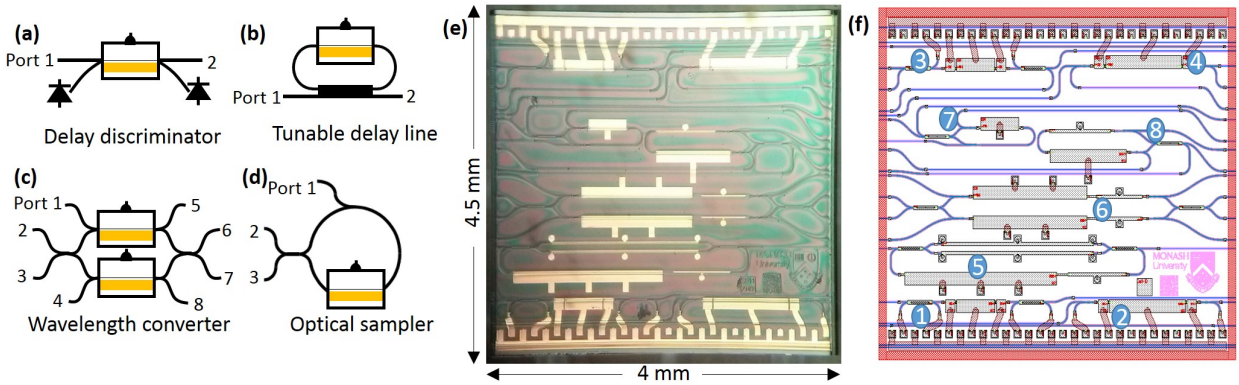

Figure 1: (a) Common topologies of active photonic circuits [2]. Arrows indicate the signal directions. (b) A photomicrograph of our PIC. (c) Mask layout. Parts (1), (3) Delay discriminator with forward-and reverse signal monitoring; (2) Delay discriminator with outwards-signal monitoring; (4) SOA with 1s2 couplers; (5) SOA in ring resonator; (6) MZI with SOAs for wavelength conversion; (7),(8) Sagnac Loop with SOA.

This work is funded by Australian Research Council Laureate Fellowship FL 130100041.

the forward pulse will saturate the gain before the backward pulse arrives. Thus, the forward pulse will have a higher power than the backward pulse, vice versa. The change in peak power transmission relies on the relative delay between the two pulses inside the device. Therefore, the PDs can give complete information of the timing delay between the pulses by monitoring the power from both sides of the device.

Figure 2 shows the differential SOA-contact voltage plotted against the actual delay. For this experiment, a pulse source from a gain-switched semiconductor is spilt into two paths using a polarization-maintaining beam splitter; each path has an adjustable 0-350 ps optical delay using tunable delay line. The two pulses enter port 1 and 2 of the SOA in Fig. 1a with different delays. The multiple crossings are due to the forwards and backwards transitions of the mirror. The result shows the sensitivity of the device to relative delay is approximately 160 μV/ps when the pulses overlap, and the differential range is approximately 40 ps.

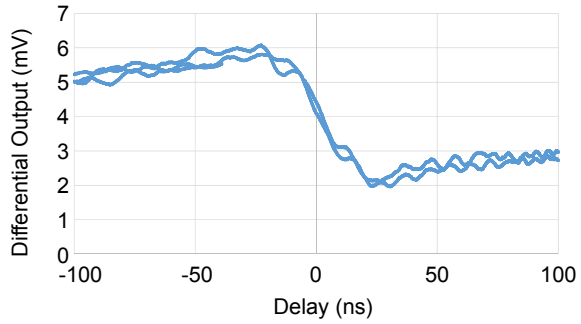

Figure 2: Waveforms showing the differential output of the SOAs versus the actual delay time [6]. (See copyright 2016, Optical Society of America)

B. *Tunable delay line*

Tunable delay lines are a key element of programmable processing functions. We used an integrated tunable delay line [7] that overcomes the delay-dependent loss, and simultaneously allows for independent manipulation of group delay and amplitude responses. This new capability is enabled by means of a ring resonator (RR) incorporates a SOA [8] in the feedback path, as shown in part 5 in Fig. 1c. By setting the SOA gain lower than the waveguide loss of the feedback path, the device provides a negative group delay at its resonant frequency in the case of undercoupling. For overcoupling, the device works as a non-minimum-phase filter allowing independent synthesis of its amplitude and group delay responses. If the SOA gain is set exactly the same as waveguide loss of the feedback path, the device works as an optical all-pass filter; such a filter provides a unity peak intensity but a positive group delay controlled by the coupling factor of the RR. Finally, when the SOA gain exceeds the overall roundtrip loss of the resonator, the resonator will be driven into laser oscillation. When tuning the SOA gain larger or smaller than the overall roundtrip loss of the resonator, and the group delay is the same and positive for both cases, this leads to attenuation or amplification of the output pulse, respectively, without changing the pulse timing. Nevertheless, the output pulse reduces to an attenuated version with a relative timing advance in negative group delay case.

Figure 3 shows the time-domain pulse measurements demonstrating the delay line function of the device in Fig. 1b. A Gaussian-envelop optical pulse train with a pulse FWHM of 5 ns and an interval of 100 ns was sent into the port 1 of Fig. 1b. Figure 3-i presents the device's group delay responses implemented in the experiment, and Fig. 3-ii shows the zoom-in view of the corresponding output pulses in the time domain. This device has been demonstrated to be able to provide a lossless delay up to 1.1 ns to a 5-ns Gaussian pulse.

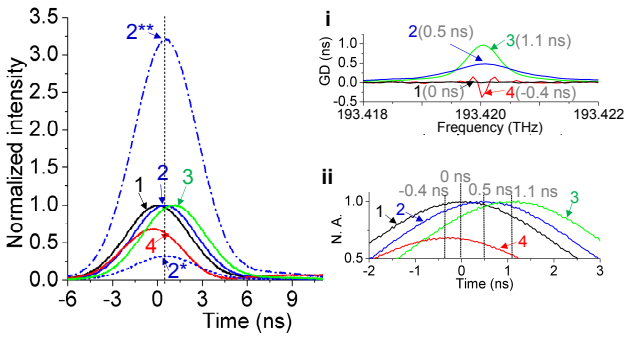

Figure 3: Demonstration of timing and amplitude variation of pulsed signals implemented using the proposed device as a tunable delay line. Insets: (i) the device's group delay responses of the pulses, (ii) zoom-in view of the output pulses. Case 1: group delay = 0 ns, 2: group delay = 0.5 ns (2* and 2** have identical delay 0.5 ns but with loss and gain, respectively), 3: group delay = 1.1 ns, 4: group delay = -0.4 ns.

C. *Wavelength converter*

All-optical wavelength converter can be used to prevent wavelength blocking in optical cross connects. Durhuus et al. [9] developed a wavelength converter based on a Mach-Zehnder interferometer with SOAs in its arms. Based on this structure, we added one phase shifter on each MZI arm, and four additional 2 × 2 couplers are added in this design, so that each SOA can be accessed directly, as shown in part 6 in Fig. 1e. A continuous wave (CW) light at the wavelength λ_1 is injected into the MZI, and at the output of the converter, it will experience constructive or destructive interference depending on the phase shift through the SOA, which depends on the bias current applied on the SOA or the input power. The optical power at λ_2 is coupled into only one SOA, the interferometer becomes unbalanced due to the saturation of one SOA and the coupling between the gain and refractive index. In this case, the phase, and thereby the output power at λ_1 will change. Therefore, a wavelength conversion is achieved. The phase shifters added in each arm are used to switch the outputs at different output ports of MZI.

Figure 4 shows the experimental results verifying the reconfigurable wavelength converter. We apply a pulse from a CW laser, λ to port 2 of the SOA-MZI device in Fig. 1c, and apply a short pulse train at 0.5-Gpulse/s to port 3 as a control signal. Untilizing cross phase modulation (XPM) and cross gain modulation (XGM) effects of the SOA plus the function of MZI converting phase change into intensity change. The waveform of control pulse is copied to the CW signal. The complementary output power at port 6 and 7 are shown in Fig. 4a and 4b. Figure 4c and 4d show the output power are switched by changing the phase on the MZI arm.

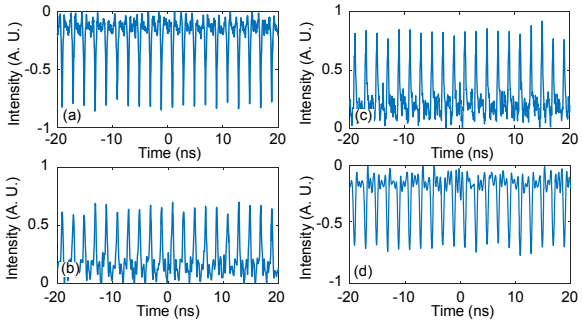

Figure 4: Measured output power at port 6 and 7 when SOA-MZI is configured that (a,b) port 6 is the copy of the waveform of control pulse, (c,d) port 7 is the copy of the waveform of control pulse.

D. Optical sampler

Sampling in the optical domain enables the time-domain demultiplexing of OTDM channels and can also be employed to reduce the receiver electronic bandwidth required for Nyquist signals [10] and optical frequency division multiplexing (OFDM) systems. Our implementation of an optical sampler is a semiconductor optical amplifier incorporated in a Sagnac loop, as shown in part 8 in Fig. 1c. [11]. Owing to cross gain modulation in the SOA and its asymmetric position in the loop, the control pulse varies the phases of the counter propagation signals at different times. In the Sagnac loop, the clockwise-travelling and counter-clockwise-travelling lights receive different amount of phase variation, depending on their iteration time with the control signal in the SOA. Eventually, by means of interference, the output coupler of the Sagnac loop translates this phase variation difference into an amplitude time gate that performs the sampling.

The input signals need to be sampled are applied to port 2 of the device in Fig. 1d, and a train of 1552-nm 5-ps pulses at 10 Gpulses/s as control pulses is inserted into the SOA via port 1. The modulating signal was generated by processing a 5 × 10 Gbaud OOK-OFDM signal through a 9-point Fourier transform, the result of which provides a modulating signal waveform characterized by eye-diagrams as shown in Fig. 5a and 5b. The eye-diagrams of the detected output from port 3 are shown in Fig. 5c and 5d. Evidently, the eyes are preserved while suppression occurs elsewhere.

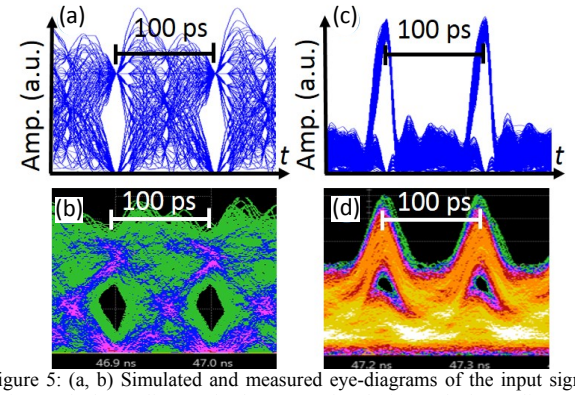

Figure 5: (a, b) Simulated and measured eye-diagrams of the input signal before optical sampling, (c, b) the output signal after optical sampling [11]. (See copyright 2016, IEEE)

IV. Conclusion

The applications of SOAs has been demonstrated in PICs for signal processors including delay discriminator, tunable delay line, wavelength converter and optical sampler.

References

[1] M. Smit and J. van der Tol and M. Hill, "Moore's law in photonics," Laser and Photon. Rev., vol. 6, pp. 1-13, January 2012.

[2] A. J. Lowery, "Active photonic integrated circuits," In Optoelectronic Devices, New York: Springer, 2005, pp. 427-448.

[3] J. Dong, X. Zhang, J. Xu, D. Huang, S. Fu, and P. Shum, "Ultrawideband monocycle generation using cross-phase modulation in a semiconductor optical amplifier," Opt. Lett., vol. 32, pp. 1223-1225, May 2007.

[4] S. Pan, X. Zhao, C. Lou, "Switchable single-longitudinal-mode dual-wavelength erbium-doped fiber ring laser incorporating a semiconductor optical amplifier," Opt. Lett., vol. 33, pp. 764-766, April 2008.

[5] A. J. Lowery, and M. Premaratne, "Reduced component count optical delay discriminator using a semiconductor optical amplifier-detector," Opt. Expr., vol. 13, pp. 290-295, January 2005.

[6] A. J. Lowery, and L. Zhuang, "Photonic integrated circuit as a picosecond pulse timing discriminator," Opt. Expr., vol. 24, pp. 8776-8781, April 2016.

[7] Y. Xie, L. Zhuang, K. J. Boller, A. J. Lowery, "Lossless microwave photonic delay line using a ring resonator with an integrated semiconductor optical amplifier," Journal of optics, vol.19, pp. 065802, May 2017.

[8] A. Rostami, H. Baghban, and R. Maram, Nanostructure semiconductor optical amplifier: building blocks for all-optical processing, Germany: Springer-Verlag, 2010, pp. 109-159.

[9] T. Durhuus, C. Joergensen, B. Mikkelsen, R. J. S. Pedersen, and K. E. Stubkjaer, "All optical wavelength conversion by SOA's in a Mach-Zehnder configuration," Photon. Technol. Lett., vol. 6, pp. 53-55, January 1994.

[10] Z. Geng, B. Corcoran, A, Boes, A. Mitchell, L. Zhuang, Y. Xie, A. Lowery, "Mitigation of Electrical Bandwidth Limitations using Optical Pre-Sampling," in OFC, pp. W2J. 6, March 2017.

[11] L. Zhuang, C. Zhu, B. Corcoran, Z. Geng, B. Song, and A. J. Lowery, "On-chip optical sampling using an integrated SOA-based nonlinear optical loop mirror," In 42nd European Conference on Optical Communication, pp. W4. P1, September 2016.